

Supplementary Information

**Multi-scale circuit model bridges molecular modeling and
experimental measurements of conductive metal-organic framework
supercapacitors**

Liang Niu^a, Zhou Liu^a, Ding Yu^a, Volker Presser^{b,c,d}, Ming Chen^a, Guang Feng^{a,*}

^a State Key Laboratory of Coal Combustion, School of Energy and Power Engineering, Huazhong University of Science and Technology (HUST), 430074 Wuhan, China

^b INM – Leibniz Institute for New Materials, Campus D2 2, 66123, Saarbrücken, Germany

^c Department of Materials Science and Engineering, Saarland University, Campus D2 2, 66123, Saarbrücken, Germany

^d saarene – Saarland Center for Energy Materials and Sustainability, Campus C4 2, 66123, Saarbrücken, Germany

*Corresponding author: gfeng@hust.edu.cn

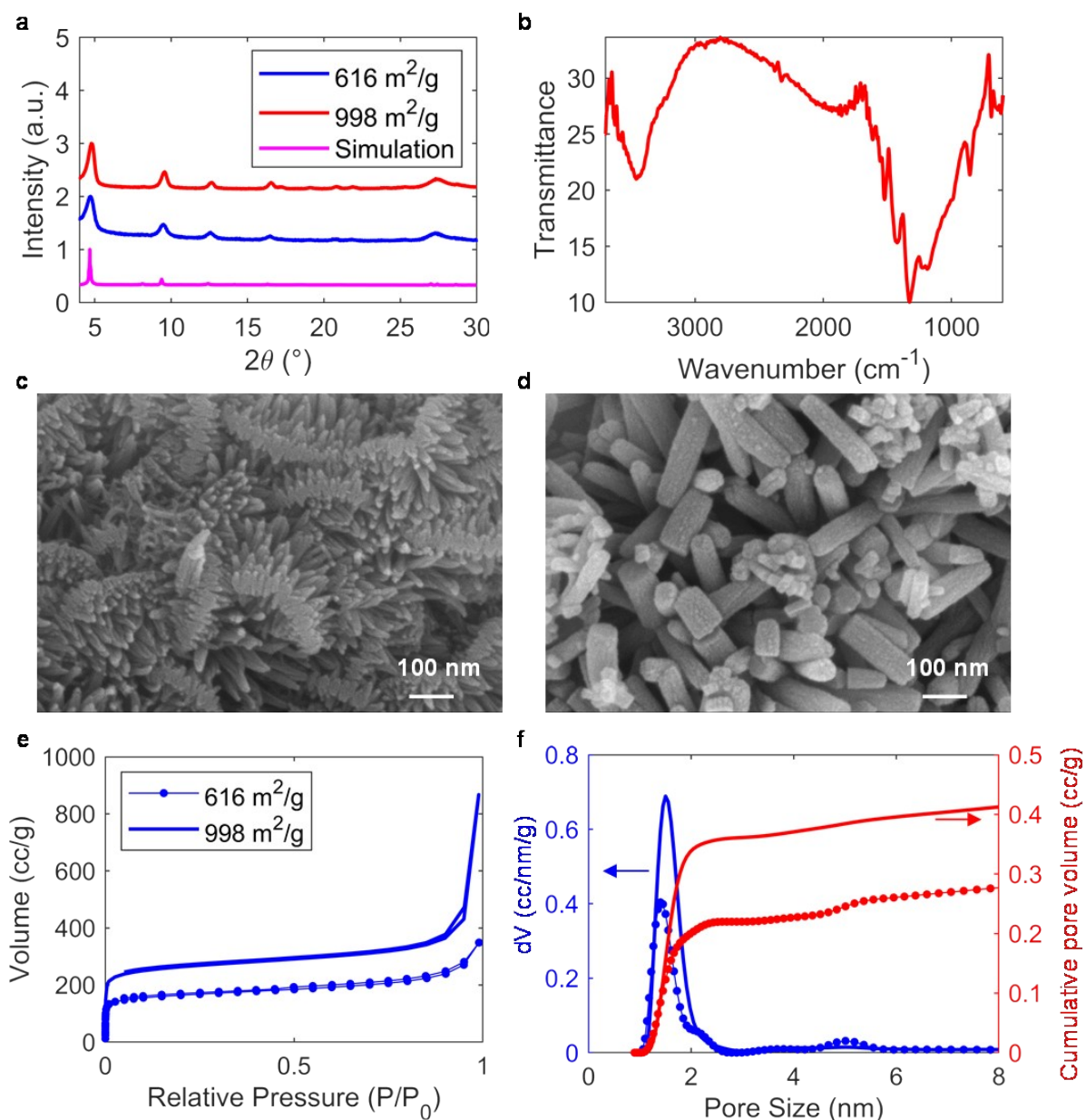


Figure S1. Characterization of conductive MOF with different SSA. **a**, Experimental and simulated XRD patterns of $\text{Ni}_3(\text{HITP})_2$. **b**, FTIR of $\text{Ni}_3(\text{HITP})_2$ with a specific surface area of $998 \text{ m}^2/\text{g}$. **c-d**, Scanning electron micrographs of $\text{Ni}_3(\text{HITP})_2$ in specific surface areas (SSAs) of **(c)**, $616 \text{ m}^2/\text{g}$ **(d)**, $998 \text{ m}^2/\text{g}$. The length and diameter of MOF with higher SSA are significantly increased while the number of rod-like crystallites is noticeably reduced. **e**, N_2 adsorption isotherm of different $\text{Ni}_3(\text{HITP})_2$ at 77 K. The SSA was computed from these isotherms as 616 and $998 \text{ m}^2/\text{g}$ using the Brunauer-Emmett-Teller method. **f**, Pore size distribution and cumulative pore volume of different $\text{Ni}_3(\text{HITP})_2$ calculated from the isotherms with the quenched solid density functional theory.

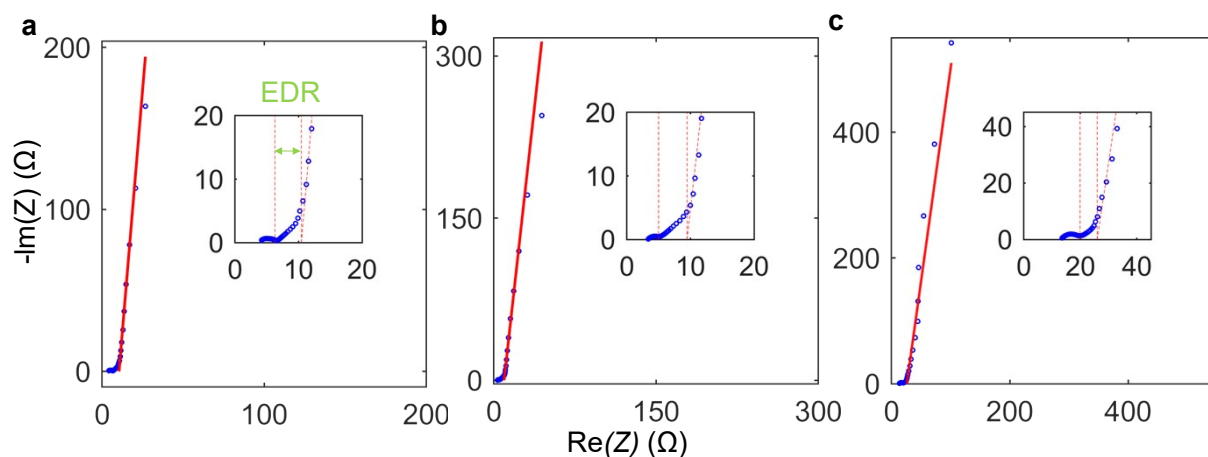


Figure S2. Nyquist plot from EIS test for c-MOF. **a-c**, Results of using a value for the crystallinity of 0.87 (a), 0.53 (b), or 0.30 (c). The method for extracting the equivalent distributed resistance is shown by the red dashed line.

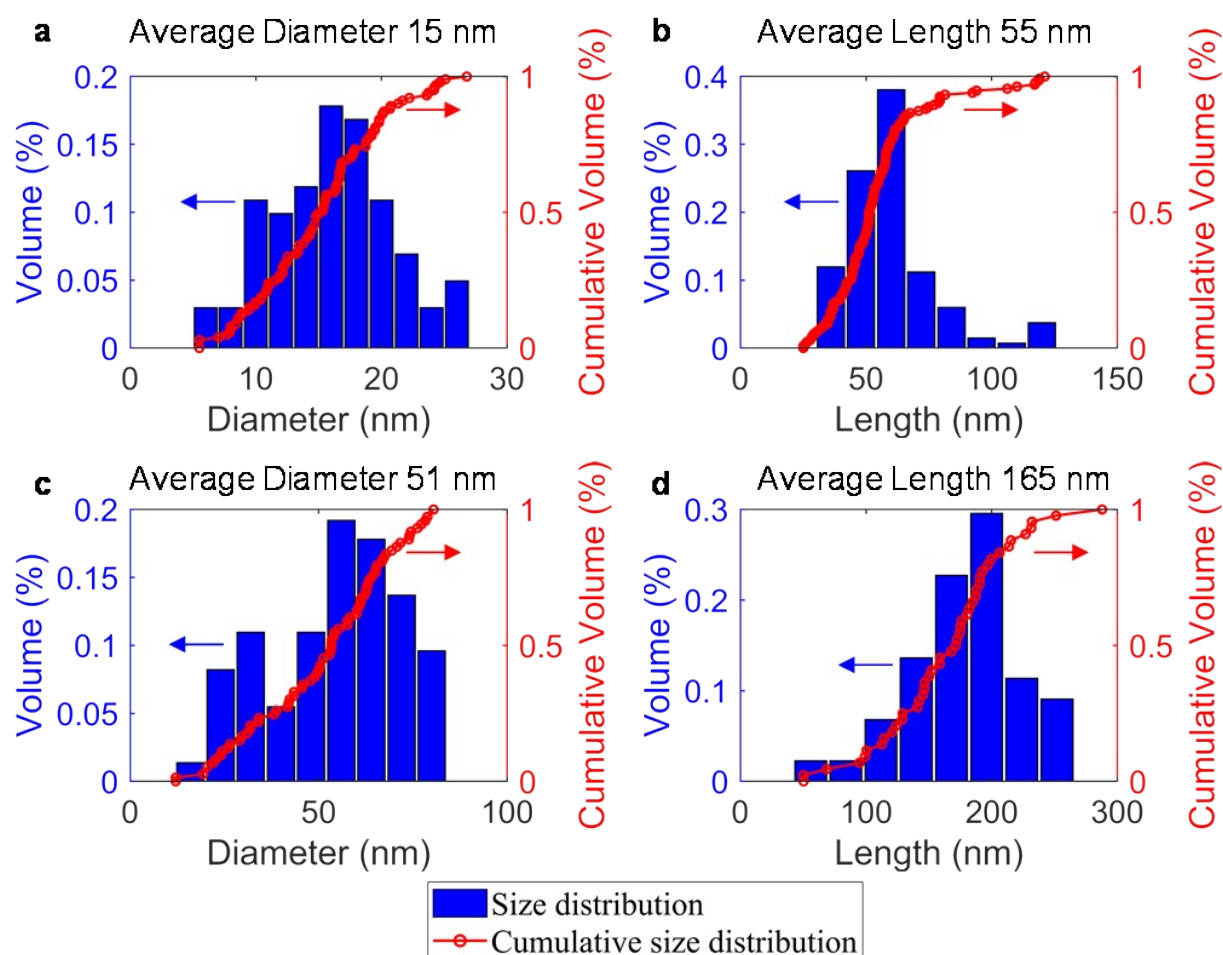


Figure S3. Diameter and Length Statistics of conductive MOF crystal rods. **a-b**, Size distribution and cumulative size distribution of $\text{Ni}_3(\text{HITP})_2$ in SSA of $616 \text{ m}^2/\text{g}$. **c-d**, Size distribution and cumulative size distribution of $\text{Ni}_3(\text{HITP})_2$ in SSA of $998 \text{ m}^2/\text{g}$.

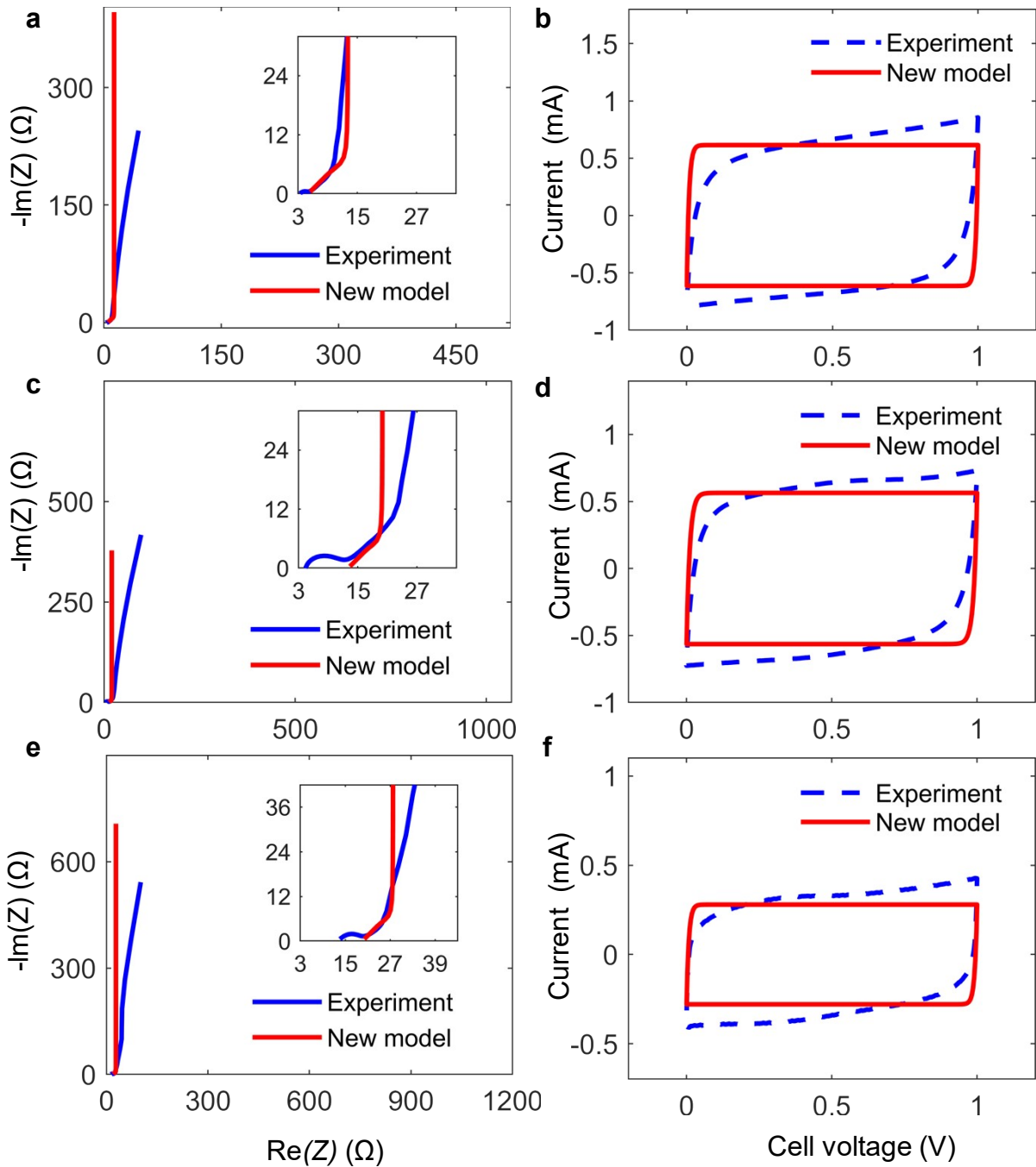


Figure S4. The comparison of the experiment to a multi-scale circuit model. Nyquist curves of experimental EIS test (blue line) and our model (red line) for samples 2-4 (a, c, e). CV curves of the experiment (blue dashed line) and multi-scale circuit model (red solid line) for samples 2-4 (b, d, f)

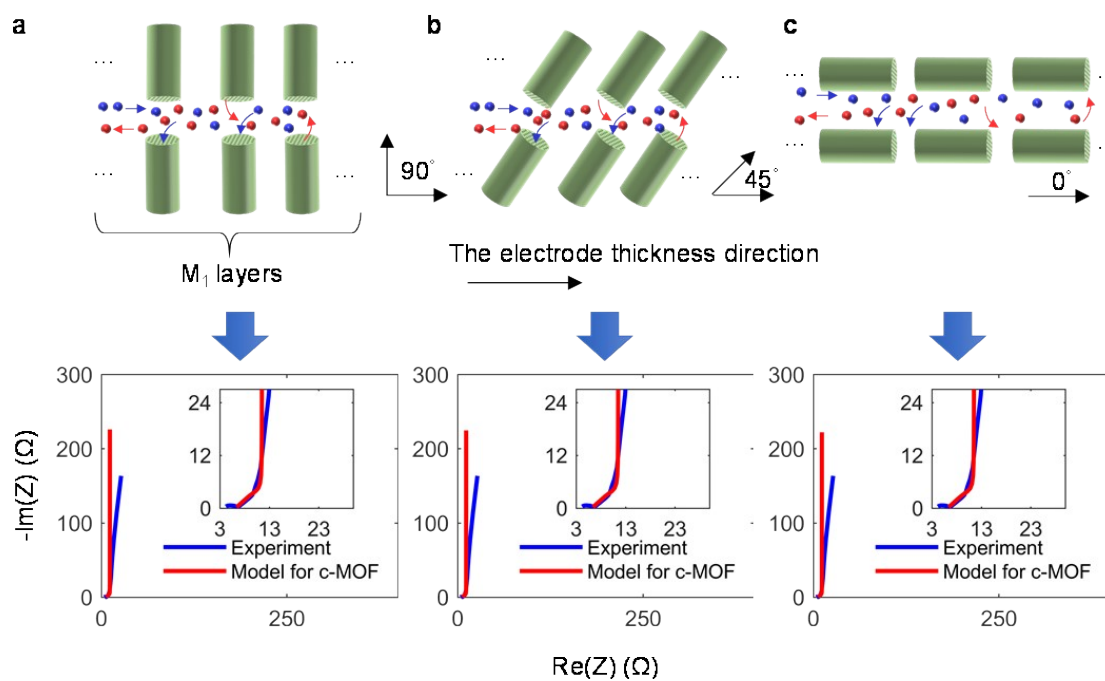


Figure S5 The influence of crystal orientation on the model's results. Schematic diagrams of crystal orientation and the corresponding Nyquist curves for the model when **a** $\alpha=1$, **b** $\alpha=1.6$, and **c** $\alpha=3.2$.

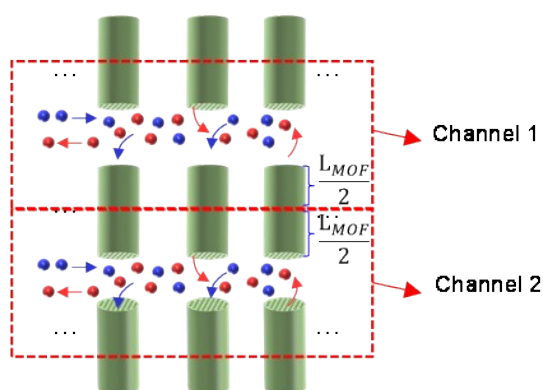


Figure S6 A schematic diagram of the relationship between the ion transport channel and the c-MOF crystal.